International Journal for Housing Science and Its Applications
Publish August 6, 2025. Volume 46, Issue 3 Pages 6339-6349

https://doi.org/10.70517/ijhsa463544

Microstructural characterization of construction asphalt mixtures using three-dimensional imaging techniques

Haocheng Xiong[1,*] and Haowen Zheng[1]
[1] School of Civil and Resources Engineering, University of Science and Technology, Beijing, 100083, China
Corresponding authors: (e-mail: 13071130135@163.com).

Abstract With the development of modern technology, three-dimensional imaging technology has been increasingly used in several fields. As a non-homogeneous material, the performance of construction asphalt mixtures is not only affected by the material composition, but also closely related to the internal structure. In this paper, the microstructural properties of construction asphalt mixtures are investigated by three-dimensional imaging technology, with the aim of exploring the relationship between aggregate distribution, void structure and asphalt-aggregate interface in asphalt mixtures. The study used 3D imaging technology to scan different types of asphalt mixtures and obtained 3D images with sub-millimeter resolution, and then analyzed their internal structural properties. The experimental results show that the distribution of coarse aggregate in dense asphalt mixtures is more uniform and the void structure is tighter, while the open-graded wearing course has larger voids and a looser structure. Through the experiments under different vacuum levels, it is found that vacuum compaction can significantly reduce the size of the voids, and the larger the vacuum level, the stronger the interfacial bond between asphalt and aggregate. Specifically, the maximum void sizes under working conditions were 15 mm and 25 mm, respectively, and the larger the vacuum degree, the smaller the proportion of large-size voids. The study shows that 3D imaging technology can effectively reveal the microstructure of asphalt mixtures, which provides data support for further optimizing the proportion and performance of asphalt mixtures.

Index Terms three-dimensional imaging technology, asphalt mixture, microstructure, aggregate distribution, void structure, interfacial bonding

I. Introduction

Construction asphalt mixtures are composed of coarse aggregates that play a role in the skeleton and fine aggregates that play a role in filling, as well as asphalt that plays a role in cementing and so on in certain proportions, is an anisotropic spatial network structure of non-homogeneous materials, and its performance is not only affected by the composition and properties of the material, but also by the influence of its composition and structure [1]-[4]. The research scales of construction asphalt mixtures can be categorized into four levels: macro, fine, micro and nano scales [5]. Traditional indoor test methods mainly study the overall characteristics and road performance of asphalt mixtures from the macro scale, which cannot reflect the spatial distribution characteristics of the components of the internal structure of asphalt mixtures [6], [7]. There are relatively few studies on the microstructure of construction asphalt mixtures such as aggregate distribution, void distribution, asphalt mastic properties, and the relationship between different microstructures and pavement performance [8]-[11].

The development of modern science and technology has promoted the continuous progress of human society, and three-dimensional imaging technology is one of them [12]. It refers to the processing of image data to generate a three-dimensional image with depth, aspect and height information, which has a wide range of applications in medicine, industry, entertainment and other fields [13], [14]. As a non-destructive testing (NDT) technique, it has been increasingly used in recent years for structural characterization of asphalt concrete, cement concrete and rock [15]. By performing NDT on asphalt mixtures, continuous tomographic image sequences with sub-millimeter resolution can be obtained, and this technique breaks through the limitations of the traditional technique, which can completely retain the three-dimensional characterization parameters such as the aggregate spatial distribution, void topology, and interfacial bonding state of construction asphalt mixtures [16]-[18].

As a key material in road construction, the performance of asphalt mixture directly affects the service life and quality of pavement. Traditionally, the research on asphalt mixtures mainly focuses on macro properties, such as compressive strength and durability. However, with the depth of research, more and more studies began to pay attention to the microstructural properties of asphalt mixtures, especially in the spatial distribution of aggregates, void structure, and the interfacial role of asphalt and aggregates. These microstructural properties not only affect

the mechanical properties of asphalt mixtures, but also have an important impact on the long-term use of pavements. In order to understand the microstructural properties of asphalt mixtures more deeply, modern three-dimensional imaging technology has gradually become an effective tool for analysis.

Traditional experimental methods, such as optical microscopy and electron microscopy, can provide some information about the microstructure of asphalt mixtures, but they are often limited by the resolution and the complexity of sample preparation. 3D imaging, on the other hand, can acquire 3D images of asphalt mixtures through non-destructive scanning, accurately displaying their internal structure and providing researchers with a more comprehensive analytical perspective. The 3D imaging technique can obtain the spatial distribution of aggregates, voids, and asphalt mastic at sub-millimeter level, and then reveal the structural differences of different types of asphalt mixtures. In this paper, the microstructural properties of asphalt mixtures were analyzed based on 3D imaging technology by obtaining 3D structural images of the asphalt mixtures. The study focuses on the aggregate distribution, void structure and interface characteristics of asphalt and aggregate of asphalt mixtures. Firstly, three common types of asphalt mixtures were selected as research objects and standardized. Then, three-dimensional imaging technology is utilized to scan them and obtain the three-dimensional images of each type of mixture under different working conditions. Finally, the spatial distribution of aggregates, the size of voids and their distribution patterns, as well as the characteristics of the interface between asphalt and aggregates were extracted by image processing technology. This study not only provides a new perspective on the microstructure of asphalt mixtures, but also provides a scientific basis for optimizing the proportioning of asphalt mixtures and improving their performance.

II. Experimental design

II. A. Selection of criteria for construction asphalt

This study to GB/T494-98 construction petroleum asphalt standards and the U.S. ASTM D312-95a roofing asphalt standards as the main product development objectives, the specific content of the standards, respectively, construction asphalt mainly on the softening point and 25 ℃ penetration of the needle degree of a higher requirement, which requires a high softening point is mainly to take into account the high temperature of the construction of asphalt in the use of high-temperature use of the performance of the asphalt in the use of the process. The requirement of high softening point is mainly to consider the construction of asphalt in the use of high temperature performance. In general, most of the construction of asphalt used in the building surface, often need to withstand direct sunlight, high temperature and other conditions of the test, high softening point can make the construction of asphalt in these conditions does not become too soft or even flow, so as to ensure that its waterproof moisture performance. Needle penetration requirements are neither too high nor too low. Too high to play the role of waterproof moisture, and too low asphalt adhesion and low-temperature performance will deteriorate. To develop a qualified construction asphalt products, asphalt products must be resolved between the needle penetration and softening point requirements of the contradiction. U.S. roofing asphalt on the product of the high and low temperature needle penetration is a higher requirement, high temperature conditions can not be too high, low temperature conditions can not be too low, the purpose of its building asphalt and the requirements of the basic similar. To develop a qualified roofing asphalt products, we must solve the product of high-temperature needle penetration is too high and low-temperature needle penetration is too low contradiction. In addition, both construction asphalt and roofing asphalt have certain requirements for ductility, the purpose of which is mainly to prevent asphalt from cracking due to deformation during use [19].

II. B. Technical properties of raw materials

For the dense asphalt concrete (AC) mix designed in this study, ordinary matrix asphalt was selected as the binder; for the asphalt-malt crushed stone (SMA), ordinary SBS-modified asphalt was selected as the binder; and for the open-graded wearing course (OGFC), high viscosity SBS-modified asphalt was used as the binder. The aggregate used in this study is pyroxene provided by a ridge crushed stone quarry, which is divided into two kinds of coarse aggregate and fine aggregate, including: 0~5, 5~10, 10~20 and 20~30mm stone chips in total 4 grades of aggregate. In order to obtain accurate and reliable test results, the aggregates were sieved one by one according to the specification of the sieve size, and then back-mixed one by one according to the design gradation.

II. C. Pilot program

II. C. 1) Surface structure design

From the three-dimensional cross-section scanning images of asphalt mixtures, it can be visualized that the factors affecting their surface structural properties are mainly: voids, aggregates and asphalt mastic components [20].

II. C. 2) Grading design

(1) type of asphalt mixture

There are major differences in the surface configuration of different types of asphalt mixtures. And different types of asphalt mixtures also have large differences in their surface skid resistance and the level of tire/pavement noise generated. Therefore, in this study, three types of asphalt mixtures commonly used in current projects are selected for experimental study, which are dense asphalt concrete mix (AC), asphalt horseshoe crushed stone mix (SMA), and porous open-graded wearing course asphalt mix (OGFC).

(2) Aggregate

(1) Nominal maximum particle size and gradation

Aggregates have a greater impact on the macroscopic structure of the mix surface, mainly the aggregate nominal maximum particle size and gradation. Therefore, for three different types of asphalt mixtures, this study selects different nominal maximum particle size of aggregates. For dense asphalt concrete, four different aggregate nominal maximum particle sizes of 17.0 mm, 13.6 mm, 9.9 mm and 4.82 mm were selected; while for asphalt mastic and open-graded wearing course mixes, three different aggregate nominal maximum particle sizes of 17.0 mm, 13.6 mm and 9.9 mm were selected. Three types of asphalt mixtures of different nominal maximum particle size under the aggregate grading design.

2) Aggregate type

Aggregate surface structure characteristics, the asphalt mixture surface microstructure has a greater impact, especially on the long-term performance of the mixture surface microstructure has a greater impact. The aggregate surface structure, on the other hand, mainly depends on the rock type of the aggregate. Therefore, in this study, in order to get a larger range of aggregate surface structure distribution, five different rock types of aggregates are selected, which are gneiss, granite, limestone, gabbro and diorite.

(3) Asphalt

The asphalt factors that affect the surface structure characteristics of asphalt mixtures are mainly asphalt type and asphalt dosage. Therefore, in order to study the effect of asphalt type on the surface structure of the mixture, two different types of asphalt were used for dense asphalt concrete mixes, matrix asphalt and ordinary SBS modified asphalt, respectively. At the same time, in order to study the effect of asphalt content on the surface structure of the mixture, three different types of asphalt mixture, are commonly used in their projects on the basis of the optimal amount of asphalt, up and down 0.5% of the oil-rock ratio, to study the effect of asphalt dosage of the surface structure of the mixture.

(4) Construction factors

In the asphalt mixture design stage, the control can be realized is the mixture compaction temperature and compaction degree. In this study, for three different types of asphalt mixtures, three different compaction temperatures and five different compaction degrees were selected. During the implementation of the specific test, the design of asphalt mixtures with different degrees of compaction was realized by changing the number of compaction times.

II. C. 3) Test flow

Based on the above test design plan, the DFT indoor test specimen panels were molded. The surface skid resistance and tire/pavement noise levels were tested separately. Then, using an automatic water jet stone cutter, the asphalt mixture specimen panels tested for skid resistance and noise level were cut into corresponding beams according to their dimensions. Using a 3D scanner, the beamlet sections were scanned. From the scanned images of the asphalt mixture sections, the internal structural parameters and surface structural indexes were analyzed and obtained. At the same time, six core samples were drilled at different parts of each asphalt mixture specimen plate as shown in Fig. 1 using an automatic water jet core drilling machine and tested for volumetric indicators.

II. D. Three-dimensional internal structure testing of asphalt mixtures

(1) Theoretical basis of three-dimensional internal structure testing

The theoretical basis for three-dimensional internal structure testing of asphalt mixtures is the principle of body vision. Stereology, as presented at an informal international conference, is a discipline based on geometric probability, statistical mathematics, differential geometry, and the theory of quartic strings and surfaces. The original definition of somatology was “the study of the relationship between three-dimensional measurements obtained from a cross-section of a tissue and the three-dimensional parameters describing that tissue”. This definition has been expanded to include the discipline of establishing the relationship between S-dimensional measurements obtained from a cross-section of a tissue and the N-dimensional parameters that describe the tissue, based on rigorous mathematical methods [21].

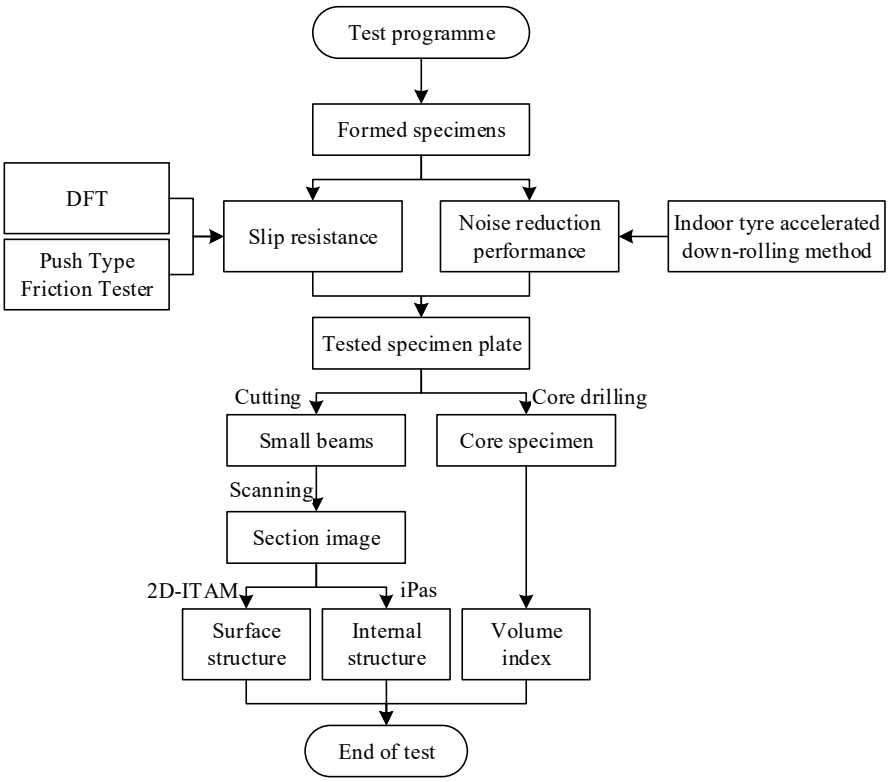

Figure 1: test process

If it is possible to obtain a sufficient number of random cross sections from an ideal organizational system (which conforms to the three basic assumptions of somatology) and calculate a sufficient number of points, line lengths, and areas, the ratio between the measured values and the values of the total organizational system is called the fractional value here for ease of presentation. Then the relationship between these measured point fraction values, line fraction values, surface fraction values and body fraction values satisfies the relationship shown in equation (1):

$$P_p = \frac{N_a}{N_T} = \frac{L_a}{L_T} = \frac{A_a}{A_T} = \frac{V_a}{V_T} \tag{1}$$

where a is the measured value, T is the total organization system value, and N, L, A and V represent the number of points, line length, area and volume, respectively.

In order to eliminate the randomness and subjectivity in the selection of parameter values during image processing, and to more objectively and accurately analyze the internal structural properties of asphalt mixtures by using cross-section scanning images, Coenen proposes the following two determination criteria:

1) The percentage of the area of the region representing coarse aggregate in the image to the total area of the mix region is the same as the percentage of the volume of coarse aggregate in the mix as measured in the laboratory.

2) The aggregate grading curve obtained in the image coincides with the aggregate grading curve measured in the laboratory.

Calculation of the volume percentage of coarse aggregate measured in the laboratory

In order to satisfy the above two determination criteria, it is first necessary to know the relationship between the quality parameters and the volume parameters of the asphalt mixture measured in the laboratory. According to the definition of density ρ and relative density γ, see equation (2):

$$\gamma = \frac{\rho}{\rho_w} \tag{2}$$

$$\rho = \frac{m}{v} \tag{3}$$

where ρ_w is the density of water, m and V are the mass and volume respectively. The asphalt volume V_b and aggregate volume V_s in the asphalt mixture can be obtained as shown in equation (4):

$$V_b = \frac{m_b}{\gamma_b \cdot \gamma_w} \tag{4}$$

$$V_s = \frac{m_s}{\gamma_s \gamma_w} \tag{5}$$

where m_b and m_s are the masses of asphalt and aggregate, respectively, and γ_b and γ_s are the relative densities of asphalt and aggregate, respectively. Then the volume of voids V_v is obtained from the proportion of volume occupied by voids in the asphalt mixture VV, as shown in equation (6):

$$VV = \frac{V_v}{V_t} \rightarrow V_v = VV \cdot V_t \tag{6}$$

where V_t is the total volume of asphalt mixture. Then the total asphalt mixture volume V_t can be expressed as equation (7):

$$V_t = V_v + V_b + V_s = VV \cdot V_t + V_s \cdot P_b \cdot \frac{\gamma_s}{\gamma_b} + V_s \tag{7}$$

where P_b is the asphalt content. Therefore, the volume percentage of aggregate in the mix P_{sv} can be expressed as equation (8):

$$P_{sv} = \frac{V_s}{V_t} = \frac{1 - VV}{P_b \frac{\gamma_s}{\gamma_b} + 1} \tag{8}$$

From the equation (8) for the calculation of the volume percentage of aggregate P_{sv}, it is clear that the calculation of P_{sv} requires the prior measurement of parameters such as the void ratio (VV) of the asphalt mixture, the asphalt content (P_b), and the relative densities of aggregate as well as asphalt, γ_s and γ_b, in the test laboratory. In order to realize the comparison with the percentage of the area of the region representing the coarse aggregate in the image to the total area of the mix region, the volume percentage of the coarse aggregate in the asphalt mixture P_{sv}^c is calculated using equation (9):

$$CF = \frac{m_c}{m_s} = \frac{V_c}{V_s} \rightarrow P_{sv}^c = \frac{V_c}{V_t} = CF \cdot \frac{V_s}{V_t} = CF \cdot \frac{1 - VV}{P_b \frac{\gamma_s}{\gamma_b} + 1} \tag{9}$$

where CF is the mass proportion of coarse aggregate in the total aggregate content.

(2) Calculation of coarse aggregate related parameters in cross-section image

The calculation of aggregate particle area in the section image of asphalt mixture is shown in equation (10):

$$A_j = N_j \cdot \Delta x^2 \tag{10}$$

where A_j is the area of the j th aggregate particle in the image, N_j is the number of pixel points that make up the aggregate particle, and Δx is the image precision, i.e. the length of a pixel point.

Once the area of the aggregate particle in the image is obtained, its equivalent circle diameter D_j^{eq} and center of the circle can be calculated as shown in Eq. (11)-Eq. (12):

$$D_j^{eq} = \sqrt{\frac{4A_j}{\pi}} \tag{11}$$

$$x_j^c = \frac{1}{N}\sum_{k=1}^{N_j} x_k,\ y_j^c = \frac{1}{N}\sum_{k=1}^{N_j} y_k \tag{12}$$

where x_j^c and y_j^c are the coordinates of their equivalent circle centers, and x_k and y_k are the coordinates of each pixel point that makes up the aggregate particle.

Then from the equivalent circle diameters of the aggregate particles, the fractional sieve balance of the aggregates in the image is calculated according to Eq. (13):

$$\text{Subtotal sieve residue}(\%) = PR_i^{im} = 100 \times \frac{A_i}{A_c} = 100 \times CF \cdot \frac{A_i}{A_c} \tag{13}$$

where A_i is the aggregate area with sieve hole size in the range i to $i+1$, equal to $\sum_{j=1}^{N_i} A_j$. j is the aggregate particle with sieve size in the range i to $i+1$, i.e. $D_i < D_j^{eq} < D_j$.

After obtaining the aggregate fractional sieve balance of each block in the image, the aggregate gradation curve obtained from the image can be plotted; and compared with the gradation curve measured in the laboratory, if the two gradation curves basically coincide, it means that the distribution characteristics of the aggregate are accurately identified from the image.

At the same time, by the principle of somatology, it can be seen that the volume percentage of coarse aggregate in the image is approximately equal to the calculated area percentage of coarse aggregate P_{sv}^{im}, as shown in equation (14):

$$P_{sv}^{im} = \frac{V_c}{V_t} \approx \frac{A_c}{A_t} \tag{14}$$

where A_c and V_c are the area and corresponding volume of the coarse aggregate in the image, and A_t and V_t are the total area and corresponding volume of the mix in the image. They are then compared with the percentage of coarse aggregate volume measured in the laboratory, and if they are the same, the area representing the coarse aggregate is considered to be accurately identified from the image.

When the above two criteria are satisfied, it can be considered that basically from the asphalt mixture section image, accurately identified the representative aggregate area. On this basis, the internal structural characteristics of asphalt mixture can be further analyzed and studied.

III. Experimental results and analysis

III. A. Analysis of parametric test results

III. A. 1) Mix uniaxial static creep test results

In recent years, for the asphalt mixture viscous - elastic - plastic characteristics of the understanding of the deepening, at room temperature under normal loading conditions asphalt mixtures are more viscoelastic. Creep is one of the important indicators to characterize the viscoelastic properties of the material, asphalt mortar due to the high content of asphalt, its creep characteristics are more worthy of consideration, asphalt mortar on the asphalt mixture creep performance is not to be ignored. In the actual wheel load process, the creep performance of mortar affects the durability of asphalt pavement. Three mortar uniaxial static creep test curve comparison shown in Figure 2.

It is generally believed that creep through the pressure density, deformation stabilization, deformation acceleration of the three stages, different stages of creep growth rate is different, respectively, from the growth of slow growth to the growth rate to maintain stable, and finally to accelerate the growth until the destruction. Creep measurement methods vary, this paper is based on uniaxial static load creep test to obtain the creep curve of different mortar at 25 ℃ room temperature conditions. Before the test starts, the specimen should be pre-pressurized according to the 10% value of the creep load to ensure that the surface of the specimen is uniformly stressed to avoid the phenomenon of eccentric stress. In this paper, the uniaxial static creep test is used to draw the creep deformation diagram of asphalt mortar, and the applied static load is 0.2P, where P is the destructive load.

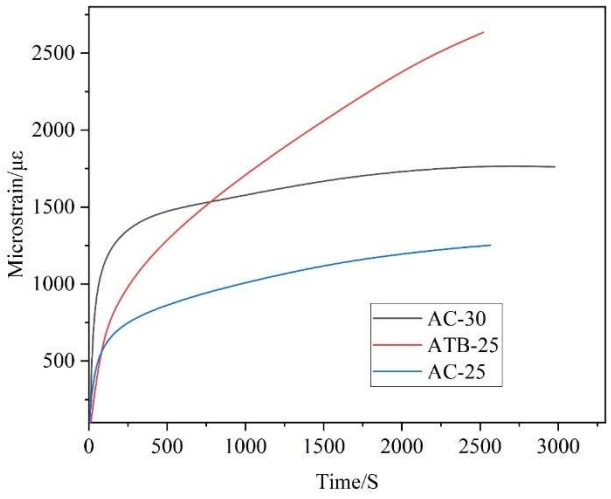

Figure 2: Three kinds of mortar single-axis static creep test curves

III. A. 2) Aggregate profile

The length and width of the smallest outer rectangle of the coarse aggregate are picked up by the digital image processing software, which represent the long and short axes of the aggregate particles, respectively, and the ratio of the short axis to the long axis can characterize the profile of the aggregate particles, and a comparison of the profile indexes of all the aggregate particles of the three grades is shown in Fig. 3. As can be seen from the figure, the three-dimensional profile of ATB-25 gradation coarse aggregate is the most reasonable, followed by AC-25 gradation and finally AC-30 gradation. The three of them are basically the same in the number of three-dimensional needle flake aggregate, which shows that the beginning end of the curve almost coincides with each other, but due to the AC-30 gradation has the largest number of coarse aggregates, its needle flake content is the lowest. However, the AC-30 gradation has the smallest amplitude of short and long axis curves, indicating that its aggregate profile is the most unreasonable.

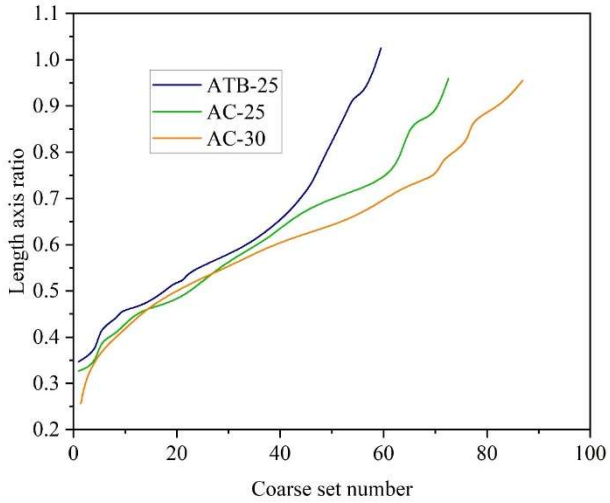

Figure 3: Three types of rough aggregate length ratio curve

III. A. 3) Characterization of aggregate composite shape

The comprehensive characterization index reflects the shape characteristics of the aggregate such as angularity, long and short axes, texture and so on. It is usually expressed by the equivalent circumference ratio, which is defined as the ratio of the actual circumference of the aggregate and the circumference of a circle equal to the area of the aggregate, and the value reflects the complexity of the boundary of the aggregate particles. If the aggregate particles are closer to round, the equivalent circumference value will be closer to 1, indicating that the aggregate is smooth and lacks corners. The equivalent circumference is calculated based on the values of perimeter and area of the aggregate obtained by the digital image processing technique, and the three gradation pairs are shown in Figure 4.

Comparison of the equivalent circumference curves of the three gradation pairs shows that the coarse aggregate in ATB-25 gradation has the best comprehensive shape index, and its aggregate boundary complexity is the highest, which is favorable for the contact between coarse aggregates to produce friction to improve the strength of the mixture; followed by AC-25 gradation, the maximum value of equivalent circumference ratio appears in this curve, but the amplitude of the curve is smaller than that of the ATB-25 gradation; similarly to the curve of the long and short axis ratio, the equivalent circumference ratio of coarse aggregate in AC-30 gradation is the same as that of ATB-25 gradation; the equivalent circumference ratio of coarse aggregate in AC-30 gradation is the same as that of AC-30 gradation. 30 gradation has the worst integrated shape characteristics of coarse aggregate, its coarse aggregate boundary is not as complex as the other two gradations, and the angularity is not rich enough. Combining the above characteristic information and the binary images of the three grades, it can be known that although the profile and integrated shape of coarse aggregate in ATB-25 gradation is the most reasonable, the binary image of its fine distribution does not form a good skeleton, and part of the mortar area is not supported by the coarse aggregate, which makes its resistance to the external force is not as good as that of the other two gradations. Comparatively speaking, AC-25 gradation and AC-30 gradation have a better skeleton structure, and most of the mortar is surrounded by coarse aggregate, forming an embedded structural skeleton protected area, which is favorable to the overall force. Therefore, the fine structural parameters affect each other, and the macroscopic mechanical response of asphalt mixture is affected by different parameters with different laws.

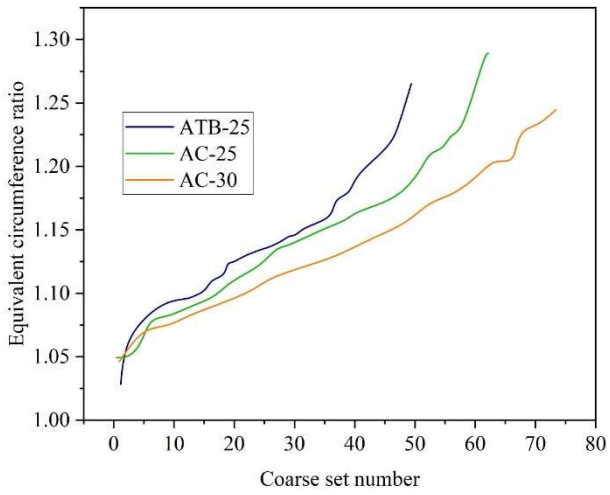

Figure 4: The equivalent circumference of three types of coarse aggregate

III. B. Analysis of test results under working conditions

III. B. 1) Test conditions

In this test, three different vacuum levels (0/-0.05MPa/-0.1MPa) and two different loading compaction devices with a total of four working conditions were selected for the study, and the working conditions were arranged as shown in Table 1.

Table 1: Test condition

	Parameter		
	Load	Vacuum (MPa)	Pressure setting
Operating condition 1	5.5kN	-0.1	Pressure setting (B)
Operating condition 2	5.5kN	-0.1	Pressure setting (A)
Operating condition 3	5.5kN	-0.05	Pressure setting (A)
Operating condition 4	5.5kN	0	Pressure setting (A)

III. B. 2) Microstructural characterization

The statistical results of void gradation and maximum void size of asphalt mixtures for different working conditions are shown in Table 2.

The percentage of voids with equivalent diameter greater than 10.2 mm and the maximum size of internal voids in asphalt mixture specimens for different conditions are shown in Fig. 5.

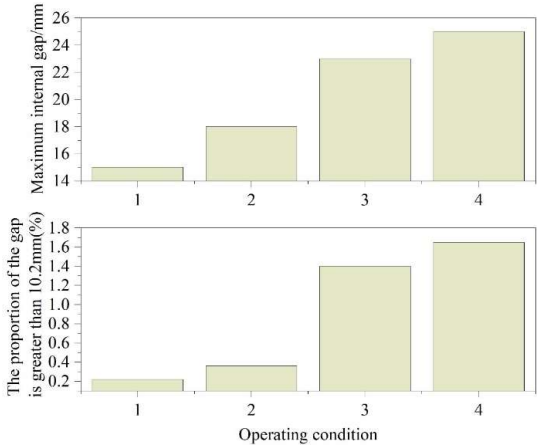

Figure 5: Analysis of the spatial gap dimensions of asphalt mixture

Table 2: Asphalt mixture void size statistics

Equivalent diameter/mm	Operating condition 1	Operating condition 2	Operating condition 3	Operating condition 4
0-0.3	2.7	2.57	7.81	7.92
0.3-0.6	22.51	18.65	13.58	14.44
0.6-0.9	14.35	11.99	10.81	11.37
0.9-1.2	14.81	12.59	9.89	10
1.2-1.5	11.24	10.76	8.24	8.04
1.5-1.8	8.33	8.78	7.13	6.71
1.8-2.1	5.5	6.04	6.16	5.46
2.1-2.4	3.76	4.42	5.2	4.69
2.4-2.7	3.14	4.14	4.23	4.03
2.7-3.0	2.76	3.58	3.51	3.63
3.0-3.3	2.23	2.94	3.23	2.93
3.3-3.6	1.71	2.28	2.66	2.44
3.6-3.9	1.2	1.88	2.16	2.11
3.9-4.2	1.22	1.62	1.95	2.08
4.2-4.5	0.96	1.35	1.73	1.76
4.5-4.8	0.78	1.06	1.5	1.4
4.8-5.1	0.66	0.89	1.35	1.37
5.1-5.4	0.58	0.78	1.19	1.07
5.4-5.7	0.44	0.68	0.92	1.05
5.7-6.0	0.38	0.54	0.72	0.78
6.0-6.3	0.32	0.44	0.81	0.82
6.3-6.6	0.32	0.43	0.65	0.61
6.6-6.9	0.28	0.32	0.63	0.66
6.9-7.2	0.27	0.27	0.59	0.55
7.2-7.5	0.22	0.24	0.41	0.45
7.5-7.8	0.18	0.18	0.45	0.41
7.8-8.1	0.17	0.19	0.31	0.36
8.1-8.4	0.16	0.12	0.35	0.38
8.4-8.7	0.13	0.15	0.3	0.35
8.7-9.0	0.12	0.12	0.24	0.28
9.0-9.3	0.13	0.07	0.26	0.23
9.3-9.6	0.12	0.11	0.28	0.26
9.6-9.9	0.1	0.07	0.21	0.17
9.9-10.2	0.08	0.07	0.18	0.23
>10.2	0.24	0.37	1.41	1.65

From the figure and table combined with the distribution of the number of voids in each condition, it can be seen that: compared with the different condition void gradation, the proportion of large-size voids in the condition 1 specimen is the smallest, 0.22%, followed by the condition 2 and condition 3 specimens, and the proportion of large-size voids in the condition 4 specimen is the largest, 1.65%. Compared with the maximum size of the voids in different conditions, the maximum size of the voids in the case 1 specimen is the smallest, 15mm, followed by the case 2 specimen and the case 3 specimen, and the maximum size of the voids in the case 4 specimen is the largest, 25mm. Explanation: Vacuum compaction can effectively reduce the size of the voids, and the bigger the vacuum, the lower the number of large-size voids, the smaller the maximum size of the voids, and the better the void microstructure is.

III. B. 3) Microstructure analysis of asphalt mixtures

In the microstructure of asphalt mixture, asphalt aggregate interface phase is different from the asphalt phase and aggregate phase, between the two phases of a thin thickness of a composite phase, it can also be argued that the interface phase region that is the interface when the damage occurs in the stressed area, asphalt and aggregate interface between the existence of tensile, pressure, shear, asphalt aggregates interface phase is mainly responsible for the stresses, the stress exceeds the limit of the strength of the interface phase of the asphalt and

the aggregates adhesion Stress exceeding the strength limit of the interfacial phase, the adhesion between asphalt and aggregate will be destroyed, and then loosening and spalling will occur. The microstructure of asphalt mixture is the root of the macro-indicators, which plays a decisive role in the indicators of the mixture's cracking resistance, water resistance, mechanical properties, and durability, etc. The analysis of the microstructure mainly focuses on the analysis of the adhesion of asphalt slurry at the interface with the aggregates, and the analysis of the micro-cracks (size/quantity). The test to four different conditions of the asphalt mixture specimens as the object of observation, using the body microscope to observe the microstructure of different conditions of asphalt mixture specimens.

Condition 4 asphalt mixture specimens of asphalt mastic-aggregate interface transition zone there are obvious cracks, cracks along the aggregate interface, the basic direction, width, distribution of continuous and obvious gaps with the aggregate surface, aggregate and asphalt mastic transition zone filled with less asphalt, poor adhesion. Asphalt mixture asphalt mastic-aggregate interface transition zone has a small width of cracks, cracks, although continuous, but cracks and aggregate surface gap is very small, compared with condition 4 specimens, aggregate and asphalt mastic transition zone filled with more asphalt, adhesion improved significantly. There are a few intermittent and not easily distinguishable cracks at the asphalt mastic-aggregate interface of the asphalt mixture, with smaller crack widths and fuzzy boundaries. Compared with Case 3, the cracks are obviously reduced, the interface between asphalt mastic and granule is full of asphalt, and the asphalt adhesion is very good. The asphalt mixture asphalt mastic-aggregate interface is well bonded, no microcracks are found, and the interface bond is compact and smooth. Compared with other conditions, the aggregate-asphalt mastic interface adhesion is the best under this condition. It can be seen that, with the increase of vacuum, the number of cracks at the asphalt mastic-aggregate interface in the asphalt mixture is obviously reduced, and the width is obviously narrowed, and it is almost not easy to distinguish the cracks when the vacuum reaches -0.1MPa. This is due to the asphalt in the “vacuum pressure” under the action of flow filling to the original location of the gap, thus improving the asphalt mastic and aggregate adhesion, with the increase of vacuum, “vacuum pressure” becomes larger, flow filling to the gap of the asphalt more, asphalt mastic and the aggregate bonding between the tighter. Aggregate bonding the tighter, the better the microscopic properties of asphalt mixtures.

IV. Conclusion

In this paper, the microstructural characteristics of asphalt mixtures were investigated using three-dimensional imaging technology, and the following conclusions were drawn:

Three-dimensional imaging technology can effectively demonstrate the aggregate distribution, void structure and the interface between asphalt and aggregate inside the asphalt mixture with high resolution and accuracy. Through the experiment, the void structure of dense asphalt mixture is more compact and the aggregate distribution is uniform, while the open-graded wearing course has larger voids and looser structure.

Through the compaction experiments with different vacuum levels, it was found that vacuum compaction can significantly reduce the proportion of large-size voids. Specifically, the proportion of large-size voids was lowest at a vacuum of -0.1 MPa, which was only 0.22%, while the proportion of large-size voids was largest at a vacuum of 0, which reached 1.65%. This indicates that vacuum compaction has a significant effect on optimizing the void structure of asphalt mixtures and improving the interfacial bonding between asphalt and aggregate.

The study shows that the interfacial bonding between asphalt and aggregate is crucial for the mechanical properties and durability of asphalt mixtures. Vacuum compaction can effectively improve the interfacial bonding and reduce the formation of microcracks, thus improving the long-term performance of asphalt mixtures.

References

[1] Gao, Y., Hou, K., Jia, Y., Wei, Z., Wang, S., Li, Z., ... & Gong, X. (2021). Variability evaluation of gradation for asphalt mixture in asphalt pavement construction. Automation in Construction, 128, 103742.

[2] Liu, N., Liu, L., Li, M., & Sun, L. (2024). A comprehensive review of warm-mix asphalt mixtures: Mix design, construction temperatures determination, performance and life-cycle assessment. Road Materials and Pavement Design, 25(7), 1381-1425.

[3] Thives, L. P., & Ghisi, E. (2017). Asphalt mixtures emission and energy consumption: A review. Renewable and Sustainable Energy Reviews, 72, 473-484.

[4] Tarsi, G., Tataranni, P., & Sangiorgi, C. (2020). The challenges of using reclaimed asphalt pavement for new asphalt mixtures: A review. Materials, 13(18), 4052.

[5] Yu, H., Dai, W., Qian, G., Zhang, C., Ge, J., & Xie, T. (2023). Research on microscopic contact characteristics of aggregates during compaction of asphalt mixtures. Construction and Building Materials, 401, 132678.

[6] Yang, B., Li, H., Zhang, H., Xie, N., & Zhou, H. (2019). Laboratorial investigation on effects of microscopic void characteristics on properties of porous asphalt mixture. Construction and Building Materials, 213, 434-446.

[7] Sun, S., Li, P., Akhtar, J., Su, J., & Dong, C. (2020). Analysis of deformation behavior and microscopic characteristics of asphalt mixture based on interface contact-slip test. Construction and Building Materials, 257, 119601.

[8] Dong, Z., Xu, G., Xu, S., Ma, S., Ma, T., Luan, Y., & Liu, J. (2024). Study on the strength composition mechanism and interface microscopic characteristics of cold recycling asphalt mixture. Frontiers in Materials, 11, 1397335.
[9] Zhao, S., Zhang, H., Gao, M., Zhang, Q., Sun, Q., & Dong, Q. (2023). Nano-microscopic analysis on the interaction of new and old asphalt mortar in recycled asphalt mixture. Chemical Physics Letters, 825, 140593.
[10] Liu, W., Gong, X., Gao, Y., & Li, L. (2019). Microscopic characteristics of field compaction of asphalt mixture using discrete element method. Journal of Testing and Evaluation, 47(6), 4579-4594.
[11] Zhao, W., Wen, W., Li, H., & Hu, J. (2024). Research on the performance of asphalt mixture with acid-treated steel slag based on microscopic properties. Construction and Building Materials, 455, 139134.
[12] Huang, Q., & Zeng, Z. (2017). A review on real‐time 3D ultrasound imaging technology. BioMed research international, 2017(1), 6027029.
[13] Zhang, S. (2021, September). High-speed 3D imaging with digital fringe projection techniques. In Tribute to James C. Wyant: The Extraordinaire in Optical Metrology and Optics Education (Vol. 11813, pp. 226-233). SPIE.
[14] Karatas, O. H., & Toy, E. (2014). Three-dimensional imaging techniques: A literature review. European journal of dentistry, 8(01), 132-140.
[15] Plati, C., Loizos, A., & Gkyrtis, K. (2020). Integration of non-destructive testing methods to assess asphalt pavement thickness. Ndt & E International, 115, 102292.
[16] Al-Mufti, R. L., & Fried, A. N. (2018). Non-destructive evaluation of reclaimed asphalt cement concrete. European Journal of Environmental and Civil Engineering, 22(6), 770-782.
[17] Apaza Apaza, F. R., Vázquez, V. F., Paje, S. E., Gulisano, F., Rodríguez, L. S., & Gallego, J. (2025). Dynamic stiffness assessment: a non-destructive testing approach for estimating density and air void content in asphalt mixtures. International Journal of Pavement Engineering, 26(1), 2499886.
[18] Meymouna, M., Bachir, G., Othmane, A., & Rabehi, R. (2023). Contribution to the non-destructive evaluation of bituminous mixes by electrical measurements. The Journal of Engineering and Exact Sciences, 9(8), 16003-01eup.
[19] Yulong Zhao,Jiaolong Ren,Ke Zhang,Yaofei Luo & Kun Wang. (2024). Construction Quality Control for Rutting Resistance of Asphalt Pavement Using BIM Technology. Buildings,14(1).
[20] Hou Lanlan,Liu Xiaofei,Ge Xinran,Hu Rongjun,Cui Zhimin,Wang Nü & Zhao Yong. (2023). Designing of anisotropic gradient surfaces for directional liquid transport: Fundamentals, construction, and applications. The Innovation,4(6),100508-100508.
[21] Kai Wang,Jiaojiao Wei,Xiaoqiang Hou & Chaoyang Wu. (2025). Evaluation of Deflection Errors in Traffic Speed Deflectometer Measurements on Inverted Asphalt Pavement Structures. Applied Sciences,15(7),4059-4059.